Defect Characterization in $ZnGeP_2$ by Time -Resolved Photoluminescence

N. Dietz[a,b], W. Busse[d], H. E. Gumlich[d], W. Ruderman[e], I. Tsveybak[e], G. Wood[b] and K.J. Bachmann[b,c]

[a]Department of Physics, [b]Department of Materials Science & Engineering, [c]Department of Chemical Engineering, North Carolina State University, Raleigh, NC 27695, [d]Technical University Berlin, and [e]Inrad, Inc., Northvale, NJ 07647

Abstract

Steady state and time-resolved photoluminescence (PL) investigations on $ZnGeP_2$ crystals grown from the vapor phase by high pressure physical vapor transport (HPVT) and from the melt by gradient freezing (GF) are reported. The luminescence spectra reveal a broad infrared emission with peak position at 1.2 eV that exhibits features of classical donor-acceptor recombination. The hyperbolic decay characteristic over a wide energy range, investigated from 1.2 eV up to 1.5eV, suggest that this broad emission band is related to one energetic recombination center. Higher energetic luminescence structures at 1.6eV and 1.7eV were revealed after annealing of $ZnGeP_2$ crystals in vacuum for a longer period of time. The emission decay behavior in this energy range is characterized by two hyperbolic time constants, viewed as the supercomposition of the decay from the broad emission center peaked at 1.2eV and additional donor-acceptor recombination emissions at 1.6eV and 1.7eV, respectively. $ZnGeP_2$ crystals grown under Ge-deficient conditions by HPVT show an additional emission structure at 1.8 eV with sharp emission fine structures at 1.778 eV related to the presence of additional donor states.

I. Introduction

Zinc germanium phosphide with a pseudodirect bandgap of ~2.1 eV at room temperature [1] has an attractive transparency range[2] from 670 nm to 13 μm and a relatively large second order susceptibility tensor component (d_{36}= 75 pm/V). In view of its substantial positive birefringence of 0.36%, $ZnGeP_2$ as a suitable material for non-linear optical applications in the infrared, e.g., the fabrication of optical parametric oscillators (OPO) and harmonic generation based on powerful infrared laser sources[3]. In addition to these and other applications in non-linear optics, $ZnGeP_2$ is of interest in the context of nearly lattice matched heteroepitaxy of compound semiconductors on silicon (a[Si] = 5.451 Å, a[$ZnGeP_2$] = 5.465 Å, c/a[$ZnGeP_2$] = 1.97) at room temperature [4].

Recently performed steady-state PL studies revealed a broad emission band with a peak maxima around 1.2 eV[5]. The origin of this broad band has remained ambiguous, especially because only the onset of this emission band was known so far. The reported changes in the high energetic shoulder were investigated as a function of composition. The observed changes in the PL spectra due to annealing or slightly off-stoichiometric growth[6-8]. They remain still valid, keeping in mind that the observed shifts of the maxima around 1.3eV might be caused by the cutoff in the photomultiplier assuming an intensity variation of the emission peaked at 1.2eV.

Even so little is known about the defect chemistry of $ZnGeP_2$ at present, electron paramagnetic resonance (EPR) measurements[9] support the strong relation of the EPR-signal with an acceptor band[10] and constricted the possible nature of the defect related acceptor band to be either Zn_{Ge} sites or V_{Zn} vacancies. From photo-induced EPR results on as grown $ZnGeP_2$ crystals, the deep PL emission is attributed to D-A transitions associated with V_P-V_{Zn} pairs[11]. However, photo-induced EPR only probes the near-surface region, while the observed optical brightening is a bulk effect. In our previous introduced defect related energy band model[5], we assign PL features to donor-acceptor (DA) recombination processes. In a DA recombination process, after generation of electron-hole pairs, the electrons and holes are captured by ionized donors and acceptors. Carriers localized at neutral donors and acceptors separated by a distance, r, may recombine radiatively emitting photons with an energy of [12]

$$h\nu = E_G - (E_D + E_A) + \frac{e^2}{\varepsilon r} - \frac{e^2}{\varepsilon}\frac{\alpha^5}{r^6} \quad (1)$$

where E_G is the band gap energy, E_D and E_A the donor and acceptor binding energies, ε the static dielectric constant and α the effective van der Walls coefficient. For very close pairs, the last term of Equ. (1) results in a series of sharp emission lines. However, a large amount of statistically distributed closely spaced pairs may broaden or even suppress the discrete emission lines due to random strain.

Results and Discussion

The energy resolved steady-state PL data in the energy range from 0.7 eV up to 2.5 eV were obtained using a combination of two liquid-N_2 cooled detectors, a GaInAs photomultiplier tube (PMT) and a Ge diode in conjunction with a 0.5 m single-grating monochromator. The excitation was accomplished by an Ar laser with excitation energies of 2.7 eV (λ= 457.8nm), 2.54 eV (λ= 488 nm) and 2.4 eV (λ= 514.8 nm) excitation lines. The system respons of the PMT was corrected to allow the combination of the two spectra, which is essential since the decreasing response of the PMT below 1.3 eV results in a false peak position of the infrared luminescence near 1.3 eV. Time-resolved PL data were obtained by a time-correlated single-photon counting technique. The excitation energy was varied by a XeCl pumped (Eximer laser λ= 308 nm) Dye laser system, Lamda EMG53MSC, in the wavelength range 460-510 nm (Coarin102). The output of the Dye laser was controlled by neutral-filters with an incident power between 100 mW and 3Watt and repetition rates between 200Hz and of 50Hz, respectively. The pulse width is in the order of 18ns. The resulting luminescence was collected and focused in a double monochromator and detected with an S-1 PMT. In lack of fast response detectors in the infrared region below 1.2 eV, the time dependence of the luminescence is carried out only in the energy range from 1.2eV up to 1.8 eV.

Figure 1 shows a typical PL spectrum for an as-grown $ZnGeP_2$ cut from a bulk single crystal grown by the gradient freezing (GF) method. The spectrum is build up from two PL spectra taken with a PMT (1.2 eV up to 2.5 eV) and a Ge-diode (0.7 eV up to 1.3 eV).

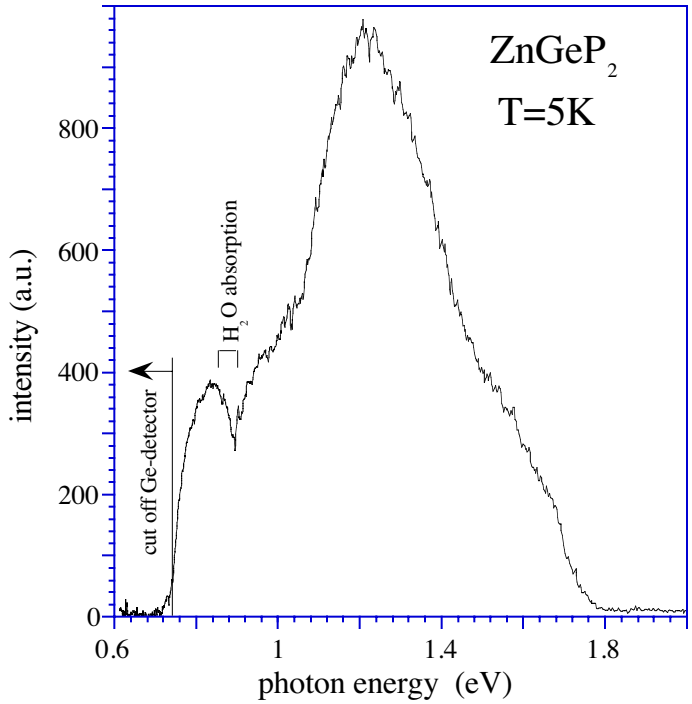

Figure 1:
Photoluminescence spectrum of bulk $ZnGeP_2$ crystal wafers that are cut from a crystal grown by gradient freezing method.

In the energy range from 1.0 eV up to 2.0 eV the spectrum is corrected with that of the PMT and the Ge-diode response function. Below 1.0 eV no correction function for the monochromator and Ge diode response was available. Thus PL spectrum is dominated by the emission peak at 1.2eV with two high energetic shoulders around 1.58 eV and 1.68 eV. The luminescence of all $ZnGeP_2$ samples show a very strong temperature dependence and no luminescence is detected at

room temperature. Figure 2 shows the temperature dependence of the PL spectrum for a $ZnGeP_2$ bulk crystal. With increasing temperature the high energetic emission around 1.6 eV and 1.7 eV decreases rapidly leaving at 100 K the 1.3 eV emission as dominant feature. The time dependence of the observed emission structures in bulk crystals is shown in Figure 3. The spectra are obtained with a S1-PMT in the single-photon counting mode and are not corrected with the PMT response characteristic. The upper curve in fig. 3 shows the emission spectrum of an annealed $ZnGeP_2$ crystal taken without a time window. The emission spectrum obtained in the time window from 0 to 100 µs mainly consists of the high energetic emission structure at 1.68 eV with a small contribution around 1.3-1.4 eV. The emission spectra taken in the time windows 0.1-2ms, 2-18ms and 18-65ms show only one emission contribution with a constant peak maximum around 1.3eV.

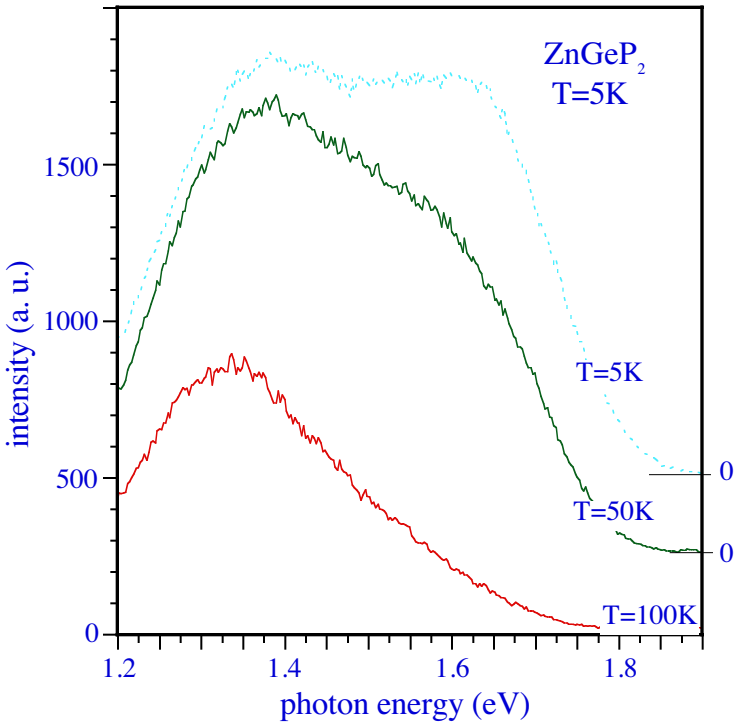

Figure 2:
Temperature dependence of the emission of a $ZnGeP_2$ bulk crystal.

This suggests that the broad emission structure at 1.3 eV is correlated to one transition center. Note, that the peak maximum position is falsed by the cutoff edge of the PMT, as indicated in fig. 1. The decay character analyzed in the energy range of 1.2eV to 1.9 eV is shown in Fig. 4 in a double logarithmic plot for the emission at 1.326 eV, 1.45 eV, 1.574 eV and 1.698 eV in curve (1), (2), (3) and (4), respectively. The decay transients in the energy range 1.2 eV up to 1.7 eV are fitted with the hyperbolic equation $I=\alpha \bullet t^{-\tau}$, with α as a pre-factor and τ the hyperbolic decay factor. The decay factor τ changes form $\tau=0.81$ at 1.326 eV to $\tau=1.0$, $\tau=1.25$ and $\tau=1.6$ at , 1.45 eV, 1.574 eV and 1.698 eV, respectively.

Crystal platelets were grown by horizontal HPVT from molten $ZnGeP_2$ sources with and without additions of excess Zn_3P_2 to cover the entire range of compositions from Ge- to Zn-rich compositions of the homogeneity range about stoichiometric $ZnGeP_2$[13] The temperature at which nucleation and growth occurred was ~35-50ºC below the melting temperature. Since the entire charge was molten and no provisions for replenishment of the molten source by the preferentially evaporating constituents was made, the composition of these platelet crystals changed from the position near to their initial nucleation sites at the fused silica wall to their peripheral parts that are formed in the final stages of growth, that is, at lower Zn partial pressure and higher density of Ge containing precursors to growth than established in the initial phase of growth. HPVT grown $ZnGeP_2$ crystals show therefore a variety of emission structures related to the different stages of growth. Figure 5 shows the photoluminescence spectra obtained in the center of a platelet with different time windows. The emission spectra are similar to that observed for bulk ZnGeP2 (Fig. 3) with one additional sharp emission peaked at 1.778 eV.

Figure 3:
Time dependence of photoluminescence of a $ZnGeP_2$ bulk crystal

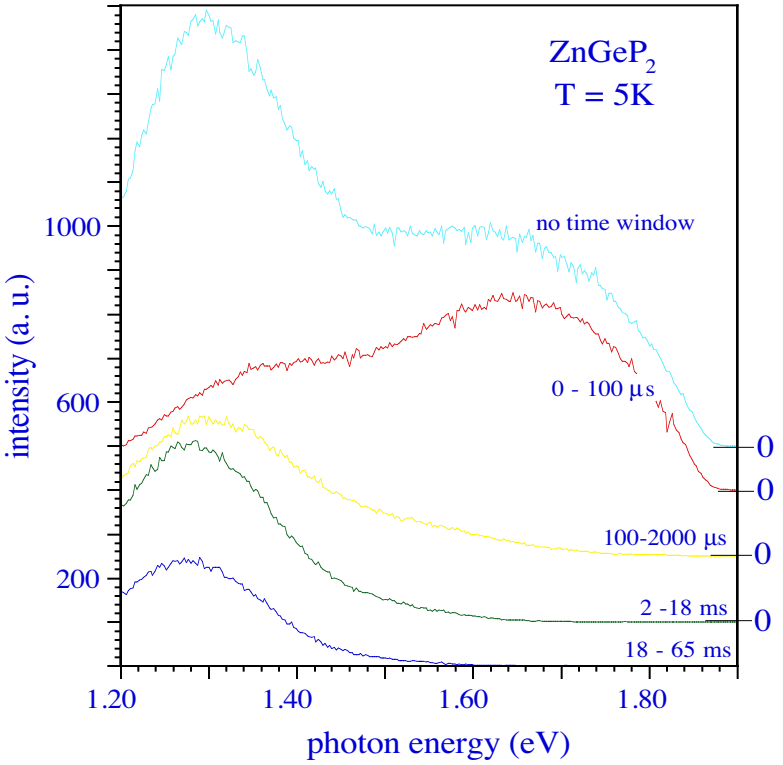

Figure 4:
Decay transients of the PL emission at 1.326 eV (1), 1.45 eV (2), 1.574 eV (3) and 1.698 eV (4). The exponent τ in the hyperbolic approximation changes form $\tau = 0.81$, $\tau = 1.0$, $\tau = 1.26$ to $\tau = 1.60$ for curve (1), (2), (3) and (4), respectively.

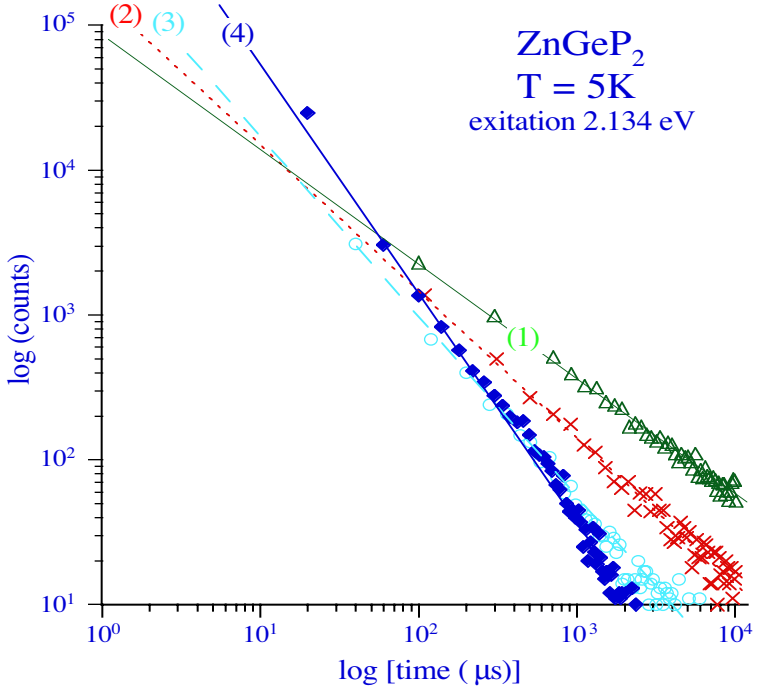

The decay time of the emission in the energy range 1.2 eV upto 1.6 eV is linear in a double logarithmic plot as shown in Fig. 6. The insert in Fig. 5 shows an enlargement of the emission around 1.778 eV with the decay time plotted in a double log. scale in the insert in Fig. 6.

Although the point defect chemistry is thus complex, hints for the predominance of certain defects are obtained by the analysis of the annealing behavior and the behavior associated with specific growth conditions. The parabolic decay time characteristic of the emission in the energy range of 1.2 eV to 1.8 eV can be interpreted in terms of transitions between donor and acceptor states associated with energy subbands in the bandgap of $ZnGeP_2$, as schematically shown in

Fig. 7. Regardless of the as-grown composition, annealing in vacuum depletes the near surface region with regard to the most volatile constituents, that is, phosphorus and zinc. The formation of vacancies on the zinc sublattice reduces the concentration of Zn_{Ge} acceptors and enhances the concentration of Ge_{Zn} donors. The introduction of V_P donors at the surface is associated with the formation of Ge_P acceptors and possibly, but not necessarily, of Zn_P acceptors. Thus the luminescence at 1.6 and 1.7 eV observed in vacuum annealed bulk crystals may be explained tentatively by transitions from V_P donors to V_{Zn}□ and Ge_P acceptors, respectively. The overall FL shift associated with the generation of V_P□ and V_{Zn}□ depends on the values of the equilibrium constants, which are not known at present. The high p-type conductivity observed upon annealing in zinc vapor, has been explained by Rud as an effect of Zn_P antisite defect formation[14]. The n-type conductivity of $ZnGeP_2$ crystals grown under HPVT suggests the formation of relatively shallow donor states that move the fermi level (FL) toward the conduction band edge. Simultaneously emission at 1.78 eV is observed that is neither seen in melt-grown crystals nor for growth from zinc-depleted vapor sources. The high phosphorus pressure used in the HPVT experiments rules out a higher V_P concentration than observed under the conditions of melt growth. Thus the donor responsible for the 1.78 eV emission for HPVT growth from a zinc supersaturated vapor phase must be associated with a different point defect that does not form for HPVT growth from zinc-depleted melt compositions.

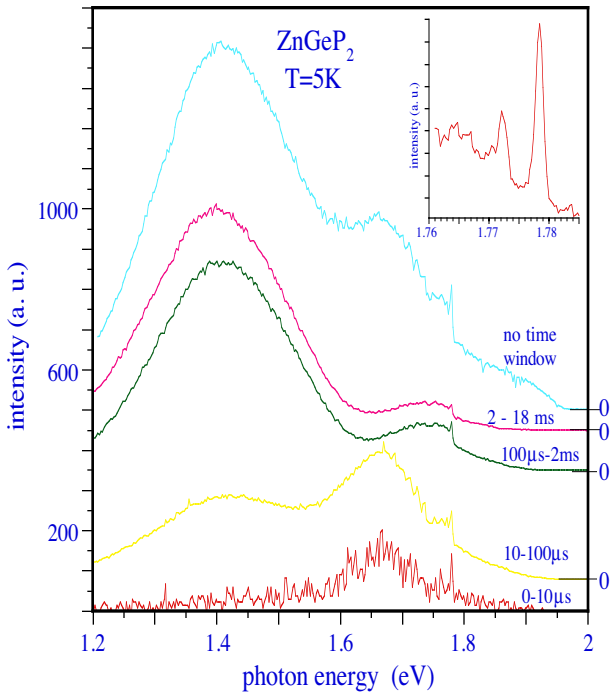

Figure 5:
Time dependence of the emission in the center of a HPVT grown $ZnGeP_2$ crystal. (Insert: Enlarged emission spectrum around 1.77 eV)

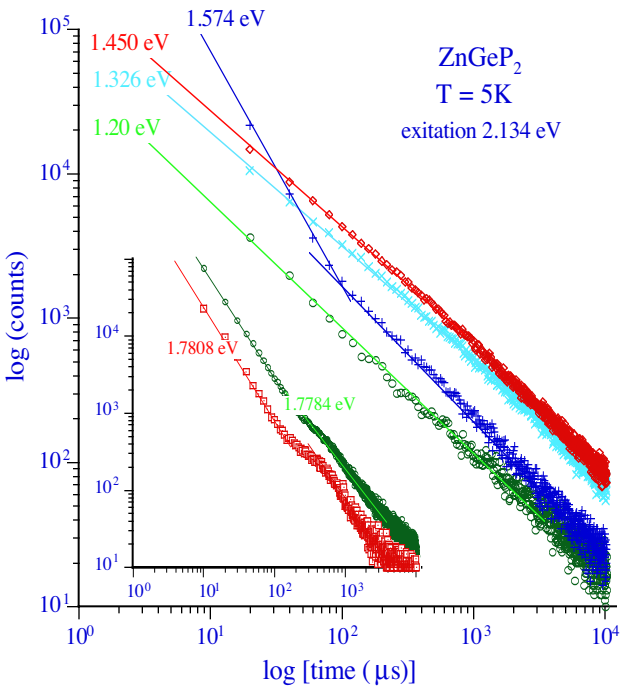

Figure 6:
Decay transients of the PL emission for a HPVT grown $ZnGeP_2$ crystals for various emission energies (Insert: Decay transients of emissions at 1.7784 eV and 1.7808 eV).

The broad deep luminescence in $ZnGeP_2$ crystals observed for crystals grown from the melt and zinc-depleted vapor sources is due to close-spaced D-A pairs , corresponding to the broad donor and acceptor subbands. Accepting the interpretation of the ENDOR measurements [15], the deep acceptor is associated with V_{zn}. Since these V_{zn} can be filled by excess Ge atoms under formation of Ge_{Zn} donors, a mechanism is identified by which Ge_{Zn}-V_{Zn} close-spaced D-A pairs can be formed. Also, we prefer the Ge_{Zn} donor over the V_P donors since the presence of Ge_{Zn} antisides upon annealing provides for the simultaneous elimination of V_{Zn} and cation disorder by the reactions (i): $Ge_{Zn} \rightarrow Ge^x + V_{zn}$ and (ii) $Zn_{Ge} + V_{zn} \rightarrow Zn^x$. The associated fermi level motion toward the conduction band edge that results in the filling of residual deep Ge_{Zn} donor states by electrons further enhances the optical brightening. Of course, the simultaneous elimination of P-

and Zn-vacancies upon annealing would be also possible, but there exists no obvious linkage in this case. Additional insights are likely to emerge from the results of irradiation studies that permit the controlled formation of defects and their characterization.

Figure 7:

Suggested model of the positions of various donor and acceptor related sub-bands in the bandgap of $ZnGeP_2$. E_{f_p} is the Fermi level for p-type and E_{f_n} the Fermi level position for n-type $ZnGeP_2$ crystals.

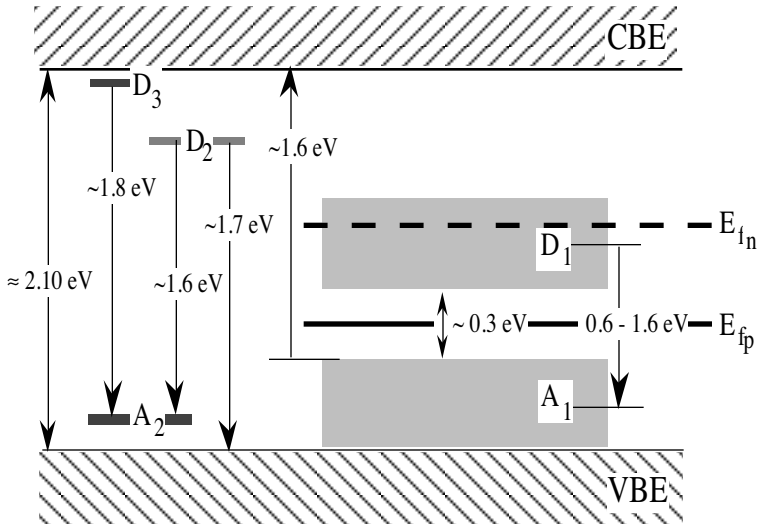

Conclusion

The native defect-related optical properties of $ZnGeP_2$ were studied by steady-state and time-resolved PL. The decay transients for the emission in the energy range 1.2 - 1.6eV show hyperbolic behavior which is interpreted as donor-acceptor pair recombination. Higher energetic luminescence structures at 1.6eV and 1.7eV were revealed after annealing of the $ZnGeP_2$ crystals. $ZnGeP_2$ crystals grown under Ge-deficient conditions by HPVT show additional emission structure at 1.8 eV and a sharp donor-acceptor emission at 1.778 eV associated to the presence of additional donor states.

References:

1. J. L. Shay and J. H. Wernick, Academic Press, New York (1976).
2. G. D. Boyd, H. M. Kasper, J. H. McFee and F. G. Storz, IEEE J. Quantum. Electron. **QE** 8, 900 (1972).
3. Y. M. Andreev, V. G. Voevodin, A. I. Gribenyukov and V. P. Novikov, Sov. J. Quantum. Electron. **17**, 748 (1987).
4. K. J. Bachmann, Mat. Res. Soc. Symp. Proc. **242**, 707 (1992).
5. N. Dietz, I. Tsveybak, W. Ruderman, G. Wood and K.J. Bachmann, Appl. Phys. Lett. **65** (22), 2759 (1994).
6. G. K. Averkieva, V. S. Grigoreva, I. A. Maltseva, V. D. Prochukhan and Y. V. Rud, phys. stat sol. (a) **39**, 453 (1977).
7. H. M. Hobgood, T. Henningsen, R. N. Thomas, R. H. Hopkins, M. C. Ohmer, W. C. Mitchel, D. W. Fischer, S. M. Hegde and F. K. Hopkins, J. Appl. Phys. **73**(8), 4030 (1993).
8. Yu. V. Rud, Semiconductors **28**(7), 633 (1994).
9. M.H. Rakowsky, W.K. Kuhn, W.J. Lauderdale, L.E. Halliburton, G.J. Edwards, M.P. Scripsick, P.G. Schunemann, T.M. Pollak, M.C. Ohmer, and F.K. Hopkins, Appl. Phys. Lett. **64**(13), 1615 (1994).
10. A. Kiel, Solid State Communications **15**, 1021 (1974).
11. N.C. Giles, L.E. Halliburton, P.G. Schunemann and T.M. Pollak, Appl. Phys. Lett. **66**, 1758 (1995).
12. J. J. Hopfield, D. G. Thomas and M. Gershenzon, Phys. Rev. Lett. **10**, 162 (1963).
13. G. Wood, Master Thesis, North Carolina State University, Raleigh NC 27695 (1994).
14. Y. V. Rud and R. V. Masagutova, Sov. Tech. Phys. Lett. **7**, 72 (1981).
15. L. E. Halliburton, G. J. Edwards, M. P. Scripsick, M. H. Rankowsky, P. G. Schunemann and T. M. Pollak, Appl. Phys. Lett. **66**, 2670 (1995).